Chin. Sci. Bull. (2014) 59(23):2898–2908
DOI 10.1007/s11434-014-0330-6

csb.scichina.com

Article

Geophysics

Distribution and origin of high magnetic anomalies at Luobusa Ophiolite in Southern Tibet

Lanfang He · Xiumian Hu · Yabing Zha · Ligui Xu · Yaohui Wang

Received: 20 August 2013 / Accepted: 11 December 2013 / Published online: 28 May 2014

Abstract The Luobusa Ophiolite, Southern Tibet, lies in the eastern portion of Indus–Yarlung Zangbo suture zone that separates Eurasia from the Indian continent. An aeromagnetic reconnaissance survey has revealed an EW-trending Yarlung Zangbo River aeromagnetic anomaly zone, and it is considered to be caused mainly by the Indus–Yarlung Zangbo Ophiolite. The Luobusa Ophiolite reflects the eastern portion of the Yarlung Zangbo River aeromagnetic anomaly zone. Conventionally, the ultramafic rock in the Luobusa Ophiolite is considered as the origin of the high magnetic anomalies. However, results from the surface magnetic survey and the magnetic susceptibility measurements from drill cores indicate that the high magnetic anomalies are distributed inhomogeneously in the Luobusa Ophiolite. In some cases, the susceptibility exhibits more than 30 times difference between two sides of the same sample. A fact emerged that the susceptibility of dunite with serpentinization is higher than that of fresh dunite, harzburgite and chromite when we analyzed the measurement results. In order to understand the origin of the high magnetic anomalies, we measured the density and susceptibility of 17 samples, microscopic and electron probe analyses have been performed as well. The result indicates the presence of dunite with serpentinization containing an abundant of micro-fissures filled with magnetite. Olivine has a susceptibility of about 2.7–351 ($\times 10^{-5}$ SI), pyroxene about 16–320, and chromite about 200–800. All these units feature relatively low susceptibility in ultramafic rock, and only the magnetite is characterized by a high susceptibility of about 200,000 ($\times 10^{-5}$ SI). Based on these observations, we conclude that the precipitation of magnetite in the process of serpentinization of the olivine caused by the geological process in the Luobusa Ophiolite is the origin of high magnetic anomalies.

Keywords High magnetic anomalies · Origin · Magnetite · Ultramafites · Luobusa · Ophiolite

1 Introduction

High magnetic anomalies (HMA), which are caused by induced or remanent magnetism, are where the measured field strength is significantly higher than the value predicted by the global model or the average value in a certain area. Their presence is ubiquitous throughout the globe [1]. How to understand and interpret such high magnetic anomalies is of great interest to geologists and geophysicists, because the cause of such anomalies is a fundamental geoscientific problem [2–5]. In addition, HMA results can also play a key role in many geological issues such as geodynamics study [6–8], tectonics research [9–11], and mineral resources prediction [12–14]. On the other hand, the geological structure and the presence of the intrusive rocks are considered to be the cause of HMA by conventional wisdom. The large-scale HMA with great spatial extents are interpreted as caused by the ophiolite formed

L. He · X. Hu
State Key Laboratory of Mineral Deposits Research, School of Earth Sciences and Engineering, Nanjing University, Nanjing 210093, China

L. He (✉) · L. Xu · Y. Wang
BGP, China National Petroleum Corporation, Zhuozhou 072750, China
e-mail: mofoo@263.net

Y. Zha
College of Information System and Management, National University of Defense Technology, Changsha 410073, China

from the subducting slab or residual of the slab along the plate suture zone, or zones of intermediate-acidic intrusive rocks [15–18]. The cause of small- or intermediate-scale HMA with minor extent is always considered as the igneous rock associated with small-scale or the local tectonic uplift [19–22]. Most regional magnetic anomalies are derived from long-wavelength data, and they reflect the characteristics of deep sources but prove difficult to verify by drilling or direct sampling. In these cases, most of magnetic anomaly interpretations rely on another method such as magnetotelluric sounding, gravity, or seismic to corroborate the result [15, 18–22]. The origin of magnetic anomalies produced by shallow buried or outcropping igneous rock can be discovered by analyzing the rock samples [23]. However, up to now, little work has been conducted on this issue. In Japan, Europe, and America, research has been carried out to study the origin of HMA of igneous rock and environmental magnetism by analyzing the magnetic rocks and minerals [24–28]. In China, the majority of similar research has focused on environmental magnetism [29–32]. Very few works are published concerning the origin of HMA based on the magnetic properties of rocks and minerals [23, 32].

The Luobusa Ophiolite (Southern Tibet) is located in the eastern portion of Yarlung Zangbo Ophiolites (Fig. 1); it is controlled by Indus–Yarlung Zangbo suture zone. Given that it hosts the largest chromitite resources in China and has perfectly outcropping ophiolite and mantle peridotite, Luobusa Ophiolite has attracted great interest of the geologists from all over the world [33, 34]. As a result, great progresses have been made on understanding its mineral characteristics [33, 35–37], deposit features [38–42], geological age of rock units, formative environment [43], and the regional tectonics [34, 44]. However, when it come to the key issues about the ophiolite, such as the origin of the rock and the chromitite, tectonic occurrence, and emplacement mechanism, there still remains debate [33, 34]. Zhou et al. [41, 42] provided a possible petrogenetic model for the formation of the Luobusa mantle sequence. In this model, the chromitites deposit is mainly formed by the interaction of water rich melt which was released from the down-going slab with the depleted harzburgite in the upper parts of the clino-pyroxene-bearing harzburgite. Research by Ren et al. [45] indicates that the peridotite recrystallized and formed the deformational coarse grained olivine, and fine grains and textures in olivine and compositional zones of chromite are preserved due to the fast cooling rate of the rock or rapid tectonic emplacement. Both of these research results consider that the mantle peridotite and the chromite within are formed in the uppermost mantle of the subduction zone. Yang et al. [46] reported the occurrence of diamond as an inclusion in Os-Ir alloy and coexist as a part of a silicate assemblage rimming grains of Fe-Ti alloy, both of which were recovered from chromitite. These evidences confirm the presence of ultrahigh pressure (UHP) minerals. These researchers proposed that the UHP minerals were incorporated into chromitites in the deep upper mantle or that these minerals have an impact origin [33, 34]. Most of the researchers accepted the emplacement model of Yarlung Zangbo Ophiolites as Tethys-type obduction [33, 34].

An HMA belt, named Yarlung Zangbo River Anomaly, is delineated by aeromagnetic studies in Tibet in 1970s and 1990s [16]. The belt includes two branches that extend about 1,400 km from west to east Tibet [16]. The Luobusa HMA lies in its north branch of the eastern portion. The width of Luobusa HMA is about 6 km based on the result of aeromagnetic studies in 1970s, which has flight altitudes varying from 2,000 to 3,000 m. In 1990s, a second aeromagnetic study with flight altitude about 1,000 m was carried out, and the result indicated the width of Luobusa HMA was about 2 km [16]. In order to analyze the distribution of Luobusa HMA and its origin, we have processed the ground magnetic survey data acquired in 2012 and measured the susceptibility of the cores from 11 boreholes. In addition, a 3D susceptibility inversion of the observed data has been conducted, and susceptibility measurements, microscopic analyses, SEM analyses of thin sections have been carried out. Based on the mineral characteristics and susceptibility values, an origin model of the high magnetic anomalies in Luobusa Ophiolite has been proposed.

2 High-accuracy ground magnetic survey in Luobusa Ophiolite

In 2012, a high-resolution ground magnetic survey was conducted in Luobusa Ophiolite, obtained an overall characterization of magnetic feature of the rock mass. Five G-858 magnetometers were used for magnetic data acquisition, and a Trimble® 5700 GPS system was used for positioning. Two types of survey grid (40 m × 20 m and 80 m × 20 m) were used in field data acquisition, and the magnetic observation accuracy is better than 0.7 nT. Fig. 2(a) shows a portion of the reduction-to-the-pole ΔT magnetic anomalies of Luobusa Ophiolite. As we can see from the figure, about 60 % of the rock mass has magnetic anomalies less than 100 nT. About 10 % of the rock mass has magnetic anomalies larger than 500 nT, and it is mainly distributed in the south of study area with a width of 100 to 400 m. A rapid 3D magnetic inversion method based on a standard geometric frame and layer-separation technique [47] was used for data inversion. This method combines fast iterative inversion with constraint inversion to obtain a robust modeling result. The fast 3D magnetic inversion

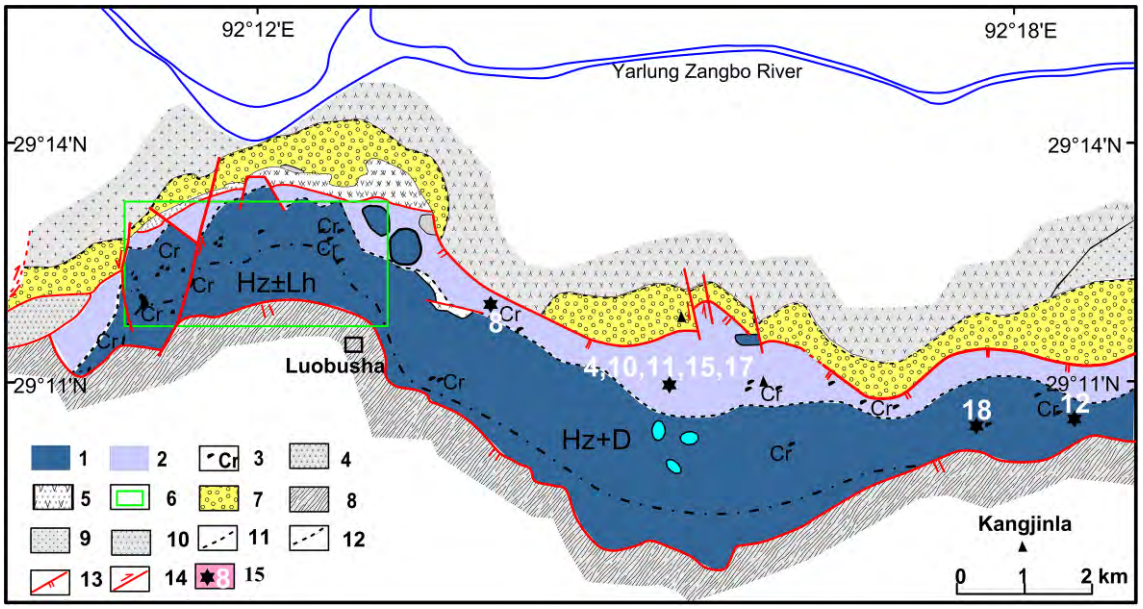

Fig. 1 Schematic geological map of the Luobusa Ophiolite (modified from Li et al. [33]). The legends are: 1, harzburgite (bearing dunite and lherzolite); 2, dunite; 3, chromitites ore; 4, cumulus bojite; 5, cumulus consist of bojite, wehrlite; 6, scope of the surface magnetic survey; 7, Luobusa group conglomerate; 8, upper Triassic Formation; 9, quartz diorite, quartz monzonite; 10, biotite granite; 11, lithostratigraphic boundary; 12, unconformable contact; 13, reverse fault; 14, strike-slip fault; 15, sample number and its position

include three algorithms, the standard geometric frame based coefficient forward modeling, the layer-separation of magnetic anomaly and the rapid inversion constrained by anomaly grid. The details of the inversion methods can be found in Yao et al. [48, 49] and Liu et al. [47, 50]. Fig. 2b displays the result of the 3D inversion, which shows that the spatial extend of HMA in Luobusa Ophiolite is limited between 200 and 400 m in depth and 100 to 400 m horizontally. The results also indicate that the distribution of magnetic susceptibility associated with the HMA in Luobusa Ophiolite is also quite inhomogeneous.

3 Susceptibility measurement of drill cores and samples

Susceptibility of 1,558 cores from 11 boreholes have been measured using the susceptibility meter ZH-1 (China Aerogeophysical Survey & Remote Sensing Center). The locations of the boreholes are shown in Fig. 2a. The lithology of drill core in Luobusa Ophiolite mainly consists of Cpx-bearing harzburgite and dunite. In order to highlight the contribution of the serpentinization to the rock susceptibility, the cores with serpentinization (including serpentine-bearing harzburgite and dunite) have been separated from Cpx-bearing harzburgite and dunite. The 1,558 cores are divided into 4 groups: (1) Cpx-bearing harzburgite (2) dunite (3) cores with serpentinization, and (4) chromitite. Two core samples are of diabase and they are not included in the statistical analyses. Note that almost all of the core samples in Luobusa Ophiolite are serpentine-bearing to various degrees. The number of core samples with serpentinization in the statistics is those in which the serpentine could be recognized by naked eyes. Table 1 lists the susceptibility of four groups: the average susceptibility of the core with serpentinization is 2654×10^{-5} SI (unless specially noted, the unit of susceptibility is 10^{-5} SI henceforth), about five times higher than the other groups. The results also show that 8 % of the susceptibility values of dunite is greater than 1,000, and 2.3 % for Cpx-bearing harzburgite, while 94.2 % of core samples with serpentinization exhibit susceptibility greater than 1,000. These values indicate that the major components of Luobusa Ophiolite, such as Cpx-bearing harzburgite and dunite, are characterized by relatively low susceptibilities, whereas the samples with serpentinization is much more magnetic and thereby contribute predominantly to the overall high susceptibility. Table 2 lists the statistics result of the core susceptibility values, and it shows that 8 percent of total core samples has a susceptibility less than 100, 64 percent ranges from 100 to 500, 17 percent from 500 to 1,000, the remaining 11 percent has a susceptibility greater than 1,000. Figure 3 shows the variation of the measured susceptibility with drilling depth and lithology. The results indicate that the core sample susceptibility varies with the lithology over a range between 30 and 32,000. Meanwhile, the result of measurements in the mine indicates that the rock susceptibility has a difference of more 30 times at two

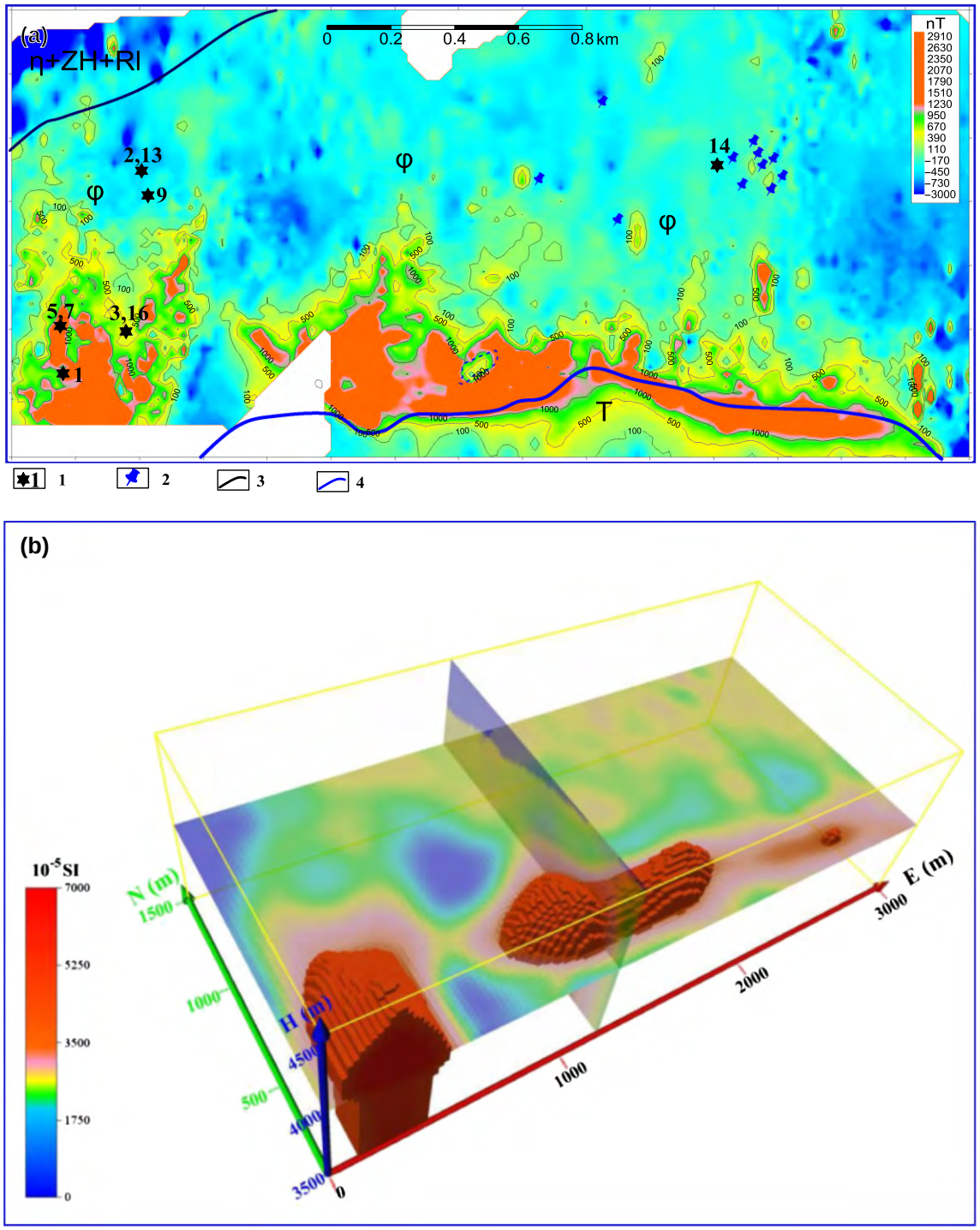

Fig. 2 Distribution of HMA in Luobusa Ophiolite (the laoction of survey area is shown in Fig. 1) **a** the reduction-to-the-pole magnetic anomaly map; **b** distribution map of 3D susceptibility inversion 1, sample position; 2, measured core susceptibility borehole location; 3, boundary of upper Triassic Formation (T) and Luobusa Ophiolite (φ), this is also the location of the fault; 4, boundary of pyroxenite, complex, conglomerate (η + ZH +RL) and Luobusa Ophiolite (φ)

locations separated by a distance of about 50 m. On different side of the same sample with a diameter of 48 mm, the difference of susceptibility is as high as 7 to 30 times (Fig. 4b and 4a, respectively). These results point to a highly inhomogeneous susceptibility variation in Luobusa Ophiolite.

In order to analyze the origin of HMA in Luobusa Ophiolite, 17 samples were collected from different parts of Luobusa

Table 1 Statistics of rock susceptibilities in Luobusa Ophiolite

Lithology	Serpentinization core	Cpx-bearing harzburgite	Dunite	Chromitites	Total
Susceptibility ($\times 10^{-5}$ SI) Mean (min–max)	2654 (409–32021)	328 (33–2935)	469 (50–3072)	338 (228–537)	
Number of sample (piece)	139	1176	228	13	1556

Table 2 Distribution of the core susceptibility

Susceptibility ($\times 10^{-5}$ SI)	10–100	10–500	500–1000	>1000	Total
Number of sample (piece)	124	996	262	176	1558

Ophiolite. Nine samples are from Luobusa Mining Areas, six from Xiangkashan, and two from Kangjingla. The sampling locations are shown in Figs. 1 and 2. The rock types range from Cpx-bearing harzburgite, dunite, magnesite, dense chromitites, scattered specks chromitites, to pea chromitites. Measurements of density, and susceptibility, as well as microscopic and SEM analyses have been carried out on the 17 samples. Susceptibility was measured using Kappabridges MFK1FA kappameter of ASC Scientific. SEM analyses were conducted in the State Key Laboratory of Mineral Deposits Research, Nanjing University by JXA-8100 electron microprobe with an analytical error around 200 ppm. Table 3 lists the result of density and susceptibility measurements. Figure 4 shows the appearance of the typical core samples. As we can see, core samples with obvious serpentine alteration (Nos. 7, 82) exhibit high susceptibility, dark-colored mineral bearing cores have relatively high susceptibility (102), fresh rock with little serpentine alteration has low susceptibility (Nos. 81 and 9). Figure 5 is the crossplot of density and susceptibility values of the 17 samples, and it shows that the susceptibility of dunite varies over the largest range, then the Cpx-bearing harzburgite, and followed by the chromitites and magnesite. Figure 6 shows the micrograph of six samples, three of them have higher susceptibility and rest have lower susceptibility. The micrograph shows that the three samples with

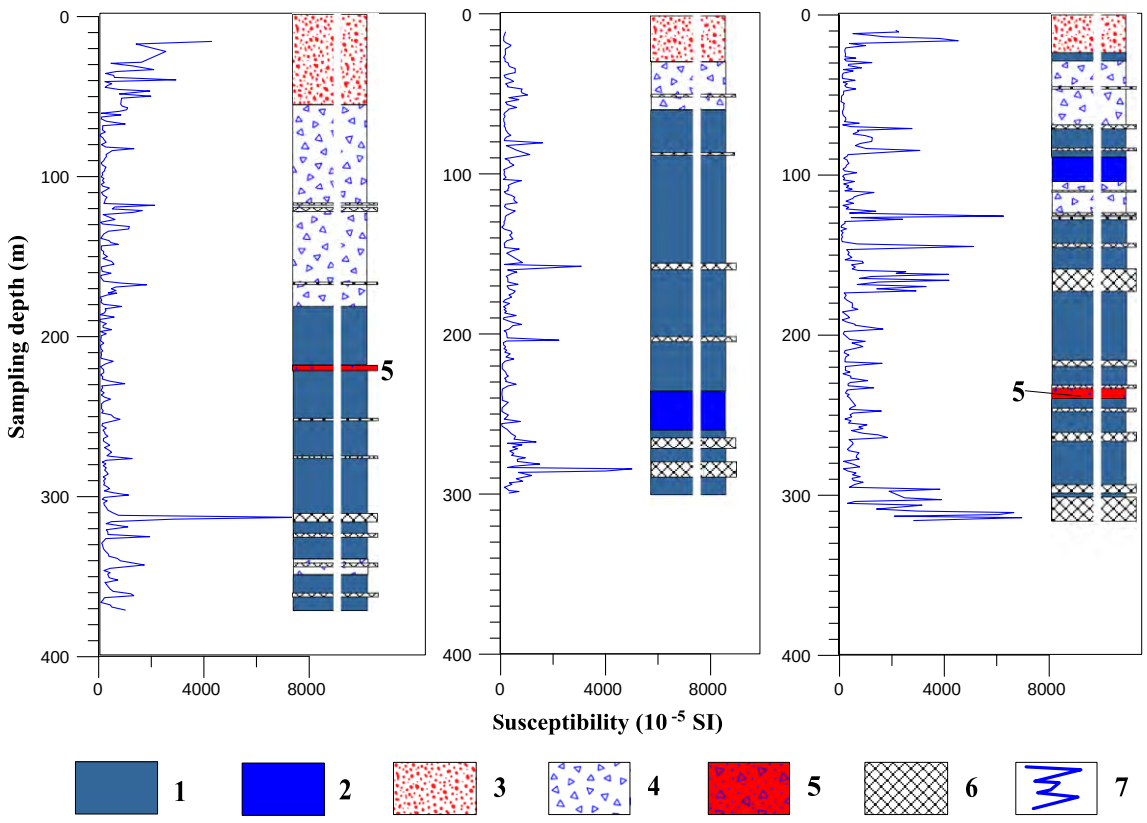

Fig. 3 Distribution of the measured core susceptibility in the borehole and its lithological column (1, Cpx-bearing harzburgite; 2, dunite; 3, slope wash, eluvium, with float of ultrabasic rock and diabase; 4, tectonic breccias which mainly consist of Cpx-bearing harzburgite and dunite; 5, chromitites-bearing layer; 6, core with serpentinization; 7, measured core susceptibility curve)

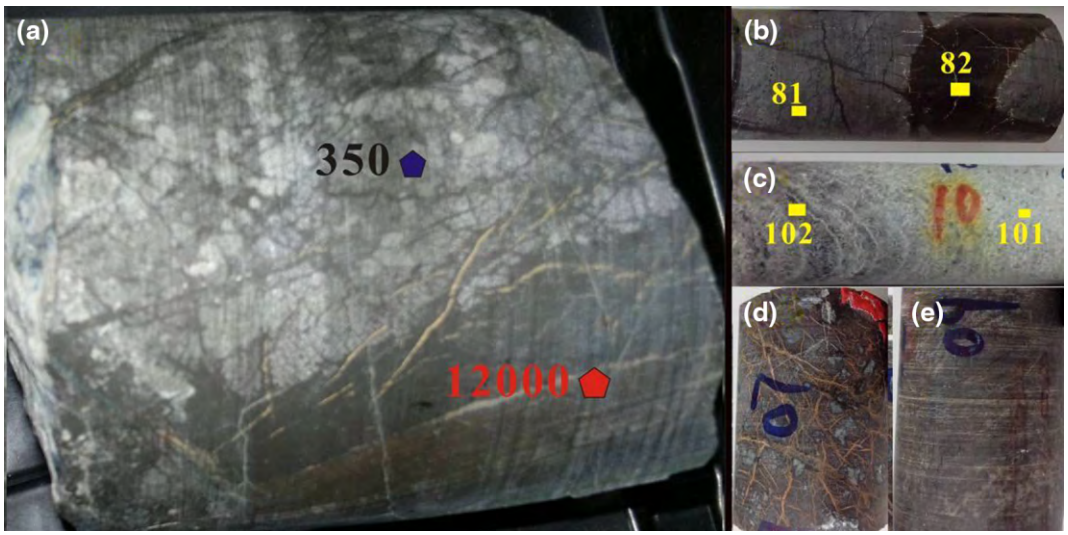

Fig. 4 Photographs of a typical 48-mm diameter core sample. **a** The difference of susceptibility values on the same core sample. The values and positions are marked in the photograph, and the data unit is (10^{-5} SI); **b** shows the measurement position (81, 82) of Sample No.8; **c** shows the measurement position (101, 102) of Sample No.10; **d** shows the serpentinization of Sample No.7; **e** is the Sample No.9, a fresh dunite

Table 3 Density and susceptibility of samples in Luobusa Ophiolite

No. of the sample	1	2	3	4	5	7	81	82	9	101
Susceptibility ($\times 10^{-5}$ SI)	3884	554	3924	2359	4649	8072	411	3422	576	109
Density (kg/m^3)	2744	2475	2777	2768	2375	2516	2913	2362	2322	2829
No. of the sample	102	11	12	13	14	15	16	17	18	
Susceptibility ($\times$ 10^{-5} SI)	546	1809	240	1234	339	1725	761	2150	1729	
Density (kg/m^3)	2730	2942	3590	2375	4047	2807	4091	2515	2700	

81, 82 from the different position of Sample No. 8; 101,102 from the different position of Sample No. 10

higher susceptibility have well developed micro-fractures filled with dark-colored minerals; the samples with lower susceptibility have almost no micro-fracture but contain cloddy dark-colored minerals. Table 4 lists the SEM analysis results, whose positions are shown in Fig. 6. The result confirms that the dark-colored minerals in the micro-fractures are magnetite and that in the cloddy is picotite. The SEM analyses also show that the picotite is enveloped by magnetite that has a thickness varying from 2 to 20 μm. The micro-fractures inside the picotite are filled with magnetite (Fig. 7).

4 Discussion

4.1 Factors influencing the HMA and susceptibility of Luobusa Ophiolite

Most magnetic surveys are carried out on the ground, and the result varies with the survey position. Apart from some areas where the rock's remanent magnetization is strong, most magnetic anomalies are caused by induced magnetization. The induced magnetization is equal to the product of the volume magnetic susceptibility and the inducing field of the earth as shown in formula (1) [51],

$$I = \kappa F. \quad (1)$$

where I is the induced magnetization, κ the volume magnetic susceptibility (dimensionless), and F the field intensity in tesla (T).

In a relatively small working area (for example, less 10 km^2), the effect of geomagnetic field and rock's remanence could be considered as a constant, the observed magnetic field intensity mainly reflect the rock's overall susceptibility. As a result, research on the feature and the origin of the rock's susceptibility could help in some way understand the distribution and the origin of HMA in a given area. The scope of the study area in Luobusa is only 2.8 km^2, and most of the observed stations lie in the Luobusa Ophiolite, so we consider the magnetic anomalies mainly vary with the variation of the rock susceptibility as a function of locations.

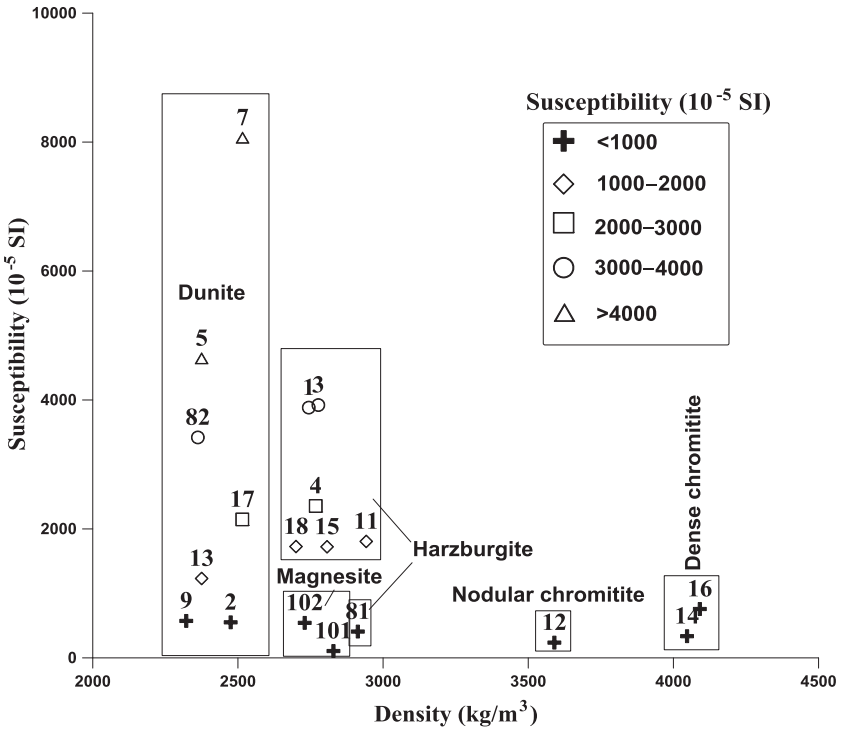

Fig. 5 Crossplot of the sample's density and susceptibility (the number in the figure is the sample code)

The susceptibility of constituent minerals and their volume or mass percentage in the rock are the major factors determining the rock's susceptibility [28, 51]. Although the main components such as olivine, pyroxene and micas are usually ferrous, they are paramagnetic. Only the iron-titanium oxide is the ferromagnetic mineral in rocks [28–32]. Tests on rock materials have shown that a rock containing 1 % magnetite may have a susceptibility as large as 1,000 times greater than that most rock materials [51]. The major rock types in Luobusa Ophiolite are Cpx-bearing harzburgite, dunite, olivine and chromitites, with primary minerals being pyroxene, olivine, chromite, and magnetite. Wang et al. [30] reported the mass susceptibility of pyroxene, olivine and magnetite as 50,000, 5 to 20, and 1 to 130 ($\times 10^{-8}$ m^3/kg), respectively. The average density of pyroxene, olivine, and magnetite is 3,200, 2,700, 4,000 kg/m^3, respectively. Therefore, we obtain the susceptibility of the three minerals as 16–320, 2.7–351, and 200,000 ($\times 10^{-5}$ SI), respectively. The measured susceptibility of chromites is 200–800. These data indicate that the main components of Luobusa Ophiolite, pyroxene and olivine, have relatively low susceptibility. Chromites in the rock also have low susceptibility. The only component of Luobusa Ophiolite that has high susceptibility is magnetite. Based on the above evidence, we conclude that magnetite in Luobusa Ophiolite is the primary contributor to the rock's overall susceptibility.

4.2 Origin of magnetite in Luobusa Ophiolite and its relation to susceptibility

Magnetite is one of the products from serpentinization process of the ferrous end member in olivine [52–54]. Zhang et al. [38] found that the magnetite in the Cpx-bearing harzburgite and lherzolite from Luobusa Ophiolite is epigenetic metasome rather than protogenous magmatic crystallization product. The average percent weight value of TiO_2 from the 14 SEM analysis test data of magnetite is 0.03 %. Based on the TiO_2–AL_2O_3–MgO ternary phase diagram [38], the presence of less than 10 % of TiO_2 also indicates that the magnetite in Luobusa Ophiolite is a type of epigenetic metasome. Photomicrographs in Fig. 6a, b, and c show that the magnetite is mainly distributed in the micro-fractures; whereas photographs of electron probe indicate that the magnetite is mainly located in the contact zone between picotite and its host olivine. The location is also consistent with the characteristics of the magnetite produced from epigenetic metasome.

Photomicrographs of six samples and SEM data (Table 3) provide a rough relationship between magnetite content and susceptibility. The susceptibility of Samples No. 7, 5 and 3, is higher than 3,000, while the photomicrographs show that the micro-fractures filled with magnetite are well developed in these three samples. From No.7 to 5 to 3, both the width of the micro-fractures and the magnetite content decrease. Correspondingly, these samples' susceptibility decreases from

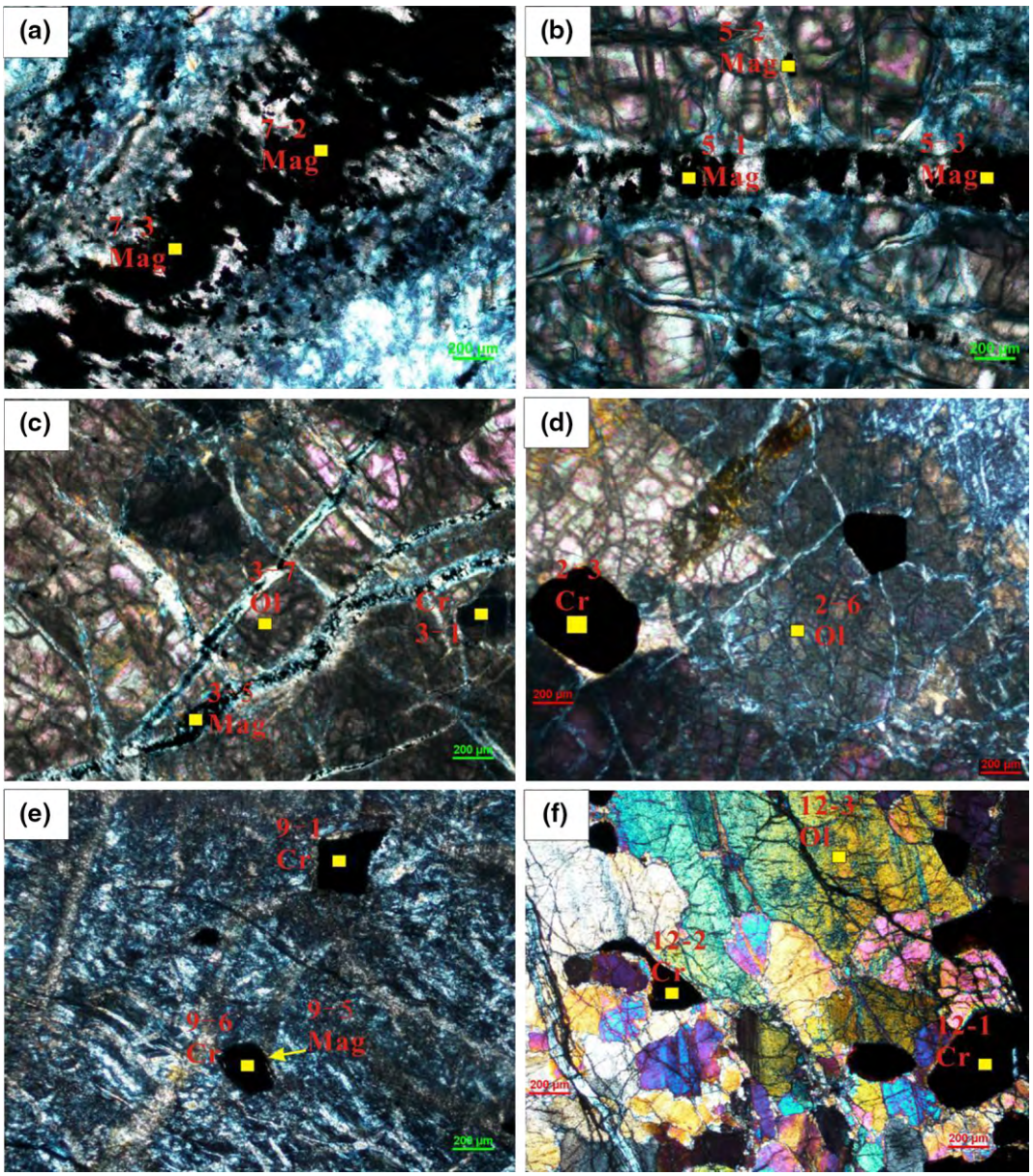

Fig. 6 Micrograph of six Samples **a** Sample No.7; **b** Sample No.5; **c** Sample No.3; **d** Sample No.2; **e** Sample No.9; **f** Sample No.12; Cr, picotite; Mag, magnetite; Ol, olivine

8072 to 4649 to 3923. Samples No. 2, 9 and 12 have susceptibility values less than 600, which are relatively low among the 17 samples. Photomicrographs show almost no micro-fractures in these three samples, and only a little magnetite surrounds the picotite in Samples No. 9 and 12. All these data indicate that the content of magnetite in Luobusa Ophiolite dominates the rock susceptibility.

4.3 Origin of the HMA in Luobusa Ophiolite

Controlled by the oxygen fugacity, the fresh Cpx-bearing harzburgite, dunite, and olivine contain little magnetite [55, 56]. The surface magnetic survey result shows that only 10 percent of the rock mass has magnetic anomalies greater than 500 nT, about 60 percent of the rock mass in Fig. 2a corresponds to low magnetic anomalies that are less than 100 nT. The susceptibility measurements indicate that more than 70 percent of core and samples have a susceptibility less than 500. It is clear that the origin of the HMA in Luobusa Ophiolite could not be generalized as the occurrence of the ultramafites. The magnetic survey has found that the HMA is mainly present in the contact zone between upper Triassic Formation (T) and Luobusa Ophiolite (φ). This zone is greatly affected by regional faulting

Table 4 SEM analysis result of the dark-colored minerals and its host rocks (wt%)

No. of sample	SiO_2	TiO_2	Al_2O_3	Cr_2O_3	FeO	MnO	ZnO	MgO	CaO	Na_2O	K_2O	NiO	V_2O_3	Total
2–3(picotite)	0.02	0.19	11.42	55.54	19.63	0.28	0.06	11.86	–	0.04	0.02	0.07	0.05	99.16
2–6(olivine)	41.16	–	–	–	5.39	0.07	–	52.87	0.07	0.05	0.05	0.23	0.05	99.95
3–1(picotite)	–	0.08	11.10	55.38	24.03	0.29	–	8.21	–	0.02	0.01	0.04	0.02	99.19
3–5(magnetite)	0.07	0.02	0.02	BL	91.40	0.07	0.05	0.19	–	0.03	–	–	0.02	91.87
3–7(olivine)	41.17	BL	BL	–	7.47	0.12	–	51.68	0.03	0.03	–	0.18	0.03	100.71
5–1(magnetite)	0.03	0.05	0.03	0.05	89.94	0.04	0.03	0.08	–	–	–	BL	–	90.25
5–2(Cr-magnetite)	1.23	0.14	2.55	22.18	64.22	2.03	0.14	1.75	–	–	–	–	0.03	94.26
5–3(magnetite)	0.02	–	–	0.00	90.20	0.06	0.09	0.08	–	–	–	–	–	90.44
7–2(magnetite)	0.02	0.05	BL	0.02	90.63	0.04	0.02	0.08	–	–	–	–	BL	90.87
7–3(magnetite)	0.03	0.02	BL	0.06	90.37	0.07	–	0.14	–	–	–	–	–	90.69
9–1(picotite)	0.01	0.20	2.60	56.78	33.61	0.49	–	4.70	BL	–	0.02	0.02	0.02	98.46
9–5(magnetite)	0.05	0.04	0.38	7.10	85.71	–	–	0.30	–	0.07	0.02	BL	BL	93.68
9–6(picotite)	0.04	0.26	12.36	54.03	20.75	0.27	0.02	11.47	0.03	0.07	0.03	0.09	BL	99.41
12–1(picotite)	0.03	0.16	11.90	58.09	14.60	0.17	–	15.09	–	–	–	0.04	–	100.08
12–2(picotite)	0.05	0.18	11.91	57.19	14.20	0.17	–	15.24	–	–	–	0.04	0.02	99.00
12–3(olivine)	40.71	–	BL	0.03	2.80	0.03	–	55.55	–	–	–	0.20	BL	99.32

SEM analysis position are shown in Fig. 6, BL means the data lower than detection limit, "–" means no data

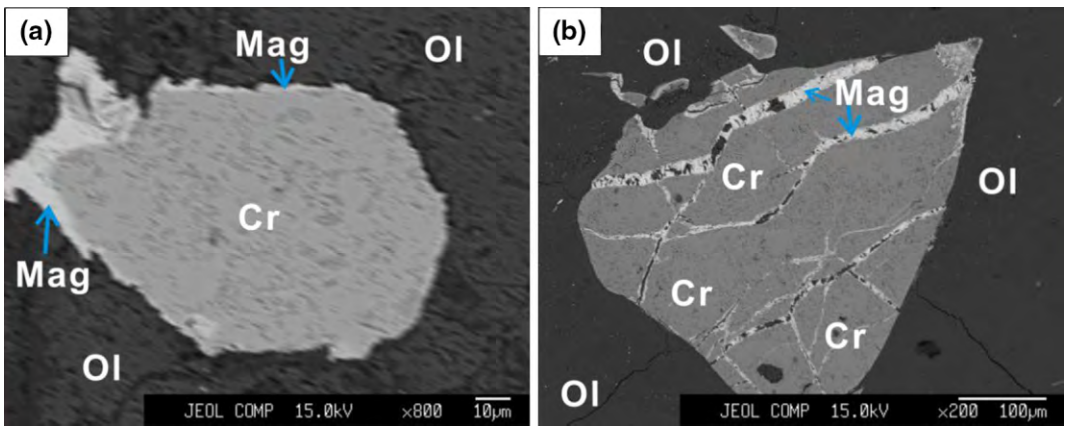

Fig. 7 Contact relation of the picotite and the magnetite (**a**, picotite is enveloped by magnetite picotite; **b**, magnetite in the micro-fractures of the picotite)

and other geological processes. Therefore, we consider faults and the geological processes related to faulting play an import role in the formation of the HMA. On one hand, the fault process deformed the ultramafic rock, and provided passage for groundwater infiltration. On the other hand, the extrusion and collision between plates provided the heat source for the alteration of the ultramafic rock. Considering the combined effect of these conditions, we surmise that the large-scale serpentinization of various degree occurred near the contact zone. Thus, we believe that the serpentinization of the olivine in the ophiolite and conversion to magnetite in this process are the origin of the HMA in Luobusa Ophiolite.

5 Conclusions

Although the aeromagnetic studies have shown that the HMA in Luobusa Ophiolite is an HMA belt, the results of surface magnetic surveys and measurement of cores and samples indicate that the distribution of HMA in Luobusa Ophiolite is highly inhomogeneous. The HMA in Luobusa Ophiolite is mainly located at the contact zone between upper Triassic Formation (T) and Luobusa Ophiolite (φ) in southern of the Ophiolite. 3D inversions of the magnetic data show that the distribution of HMA source in Luobusa Ophiolite is limited in depth between 200 and 400 m, which is a kind of shallow source HMA. Results from core and

sample analyses show that cores or samples with high susceptibility have visible macroscopic serpentinization, while microscopic and SEM analyses confirmed that magnetite fills the micro-fracture in the samples. The major composition difference between the samples with high and low susceptibility is the content of magnetite, and the amount and distribution of the exsolution of magnetite in the process of the serpentinization of the olivine in the ophiolite mainly contribute to the HMA and its spatial distribution. We conclude that the serpentinization of the olivine in the ophiolite and rock exsolution of magnetite in the geological process, especially the tectonics, account for the origin of the HMA in Luobusa Ophiolite.

Acknowledgments Great thanks to Prof. Lihui Chen, Wenlan Zhang, doctoral candidate Wei An and Yaoming Xu from Nanjing University, Dr. Jiangang Wang from Chinese Academy of Sciences, Prof. Rujun Chen and postgraduate Yu Cui from Central South University, Yunxiang Liu, Jingming Song, Heqiang Dai from BGP, CNPC, for their help in data measurement, analysis and processing. This work was supported by the National Natural Science Foundation of China (U1262206), Chinese Geological Survey Geological Prospecting Fund (12120113095200) and the National Science and Technology Program (2011ZX05019-007).

References

1. Reeves C (2008) The first magnetic anolmaly map of the world. Lead Edge 27:32–33
2. Varne R, Gee RD, Quilty PG (1969) Macquarie Island and the cause of oceanic linear magnetic anomalies. Science 166:230–232
3. Liu QS, Gao S, Zheng JP (1998) Research on the magnetic structure of continental crust and its significance. Chin Sci Bull (Chin Ver) 43:1246–1252 (in Chinese)
4. Zhang CD (2013) Models of the earth's lithospheric magnetic field and their application (in Chinese). Geophys Geochim Explor 31:1–10
5. Vaughan AP, Wareham CD, Johnson AC et al (1998) A Lower Cretaceous, syn-extensional magmatic source for a linear belt of positive magnetic anomalies: the Pacific Margin Anomaly (PMA), western Palmer Land, Antarctica. Earth Planet Sci Lett 158:143–155
6. Liang RC, Pei YL, Zheng YP et al (2003) Gravity and magnetic field and tectonic structure character in the southern Yellow Sea. Chin Sci Bull 48(Suppl):64–73
7. Li CF, Zhou ZY, Hao HJ et al (2008) Late Mesozoic tectonic structure and evolution along the present-day northeastern South China Sea continental margin. J Asian Earth Sci 31:546–561
8. Gorodnitskiy AM, Brusilovskiy YV, Ivanenko AN et al (2013) New methods for processing and interpreting marine magnetic anomalies: application to structure, oil and gas exploration, Kuril forearc, Barents and Caspian seas. Geosci Front 4:73–75
9. Abedi M, Gholami A, Norouzi GH (2013) A stable downward continuation of airborne magnetic data: a case study for mineral prospectivity mapping in Central Iran. Comput Geosci 52:269–280
10. Pilkington M, Saltus RW (2009) The Mackenzie River magnetic anomaly, Yukon and Northwestterritories, Canada—evidence for early proterozoic magmatic arc crust at the edge of the North American craton. Tectonophysics 478:78–86
11. Surinach E, Galindo-zaidivar J, Maldonado A (1997) Large amplitude magnetic anomalies in the northern sector of the Powell Basin, NE Antarctic peninsula. Mar Geophys Res 19:65–80
12. Kang GF, Gao GM, Bai CH et al (2012) Characteristics of the crustal magnetic anomaly and regional tectonics in the Qinghai-Tibet Plateau and the adjacent areas. Sci China Earth Sci 55:1028–1036
13. Li CF, Song TR (2012) Magnetic recording of the Cenozoic oceanic crustal accretion and evolution of the South China Sea basin. Chin Sci Bull 57:3165–3181
14. Wang PX (2012) Tracing the life history of a marginal Sea-On the "South China Sea Deep" Research Program. Chin Sci Bull 57:3093–3114
15. Mishra DC, Kumar VV, Rajasekhar RP (2006) Analysis of airborne magnetic and gravity anomalies of peninsular shield, India integrated with seismic and magnetotelluric results and gravity anomalies of Madagascar, Sri Lanka and East Antarctica. Gondwana Res 10:6–17
16. Yao ZX, Zhou FH, Xue DJ et al (2001) The property of the Yarlunag Zangbo River Areomagnetic anomaly zone and its significance. Geophys Geochim Explor 25:241–252 (in Chinese)
17. Rybakov M, Goldshmidt V, Hall JK et al (2011) New insights into the sources of magnetic anomalies in the Levant. Russ Geol Geophys 52:377–397
18. Kostadinoff J, Bjerg EA, Gregori D et al (2001) Magnetic and gravity anomalies in the Sierra del Padre and Sierra del Tala, San Luis Province, Argentina: Evidence of buried mafic–ultramafic rocks. J South Am Earth Sci 14:271–276
19. Quesnel Y, Weckmann U, Ritter O et al (2009) Simple models for the beattie magnetic anomaly in South Africa. Tectonophysics 478:111–118
20. Molnar P, Atwater T, Mammerickx J et al (1975) Magnetic anomalies, Bathymetry and the tectonic evolution of the South Pacific since the late Cretaceous. Geophys J Res 40:383–420
21. Hu DK, Zhou D, Wu XJ et al (2008) Origin of high magnetic anomaly belt in northeastern South China Sea as indicated by geophysical inversion. J Trop Oceanogr 27:32–37 (in Chinese)
22. He BZ, Jiao CL, Cai ZH et al (2011) A new interpretation of the high aeromagnetic anomaly zone in central Tarim Basin. Geol Chin 38:961–969 (in Chinese)
23. Lang YQ, Hu DQ, Liu C et al (2011) Mineralogy study of magnetic susceptibility of rocks along the coast of the northern South China Sea. Chin J Geophys 54:573–587 (in Chinese)
24. Butler RF, Banerjee SK, Stout JH (1976) Magnetic properties of oceanic pillow basalts: evidence from Macquarie Island. Geophys J Int 47:179–196
25. McEnroe SA, Langenhorst F, Robinson P et al (2004) What is magnetic in the lower crust? Earth Planet Sci Lett 226:175–192
26. Piper JD, Mallik SB, Bandyopadhyay G (2003) Palaeomagnetic and rock magnetic study of a deeply exposed continental section in the Charnockite Belt of southern India: implications to crustal magnetisation and palaeoproterozoic continental nuclei. Precambrian Res 121:185–219
27. Xu HJ, Jing ZM, Ou XG (2004) Effects of retrogression of ultrahigh-pressure eclogites on magnetic susceptibility and anisotropy. Earth Sci J China Univ Geosci 29:674–684
28. Liu YY (1984) Rock's magnetism. Geol Sci Technol Info 3:81–85 (in Chinese)
29. Zhou LP, Oldfield F, Wintle AG (1990) Partly pedogenic origin of magnetic variations in Chinese Loess. Nature 346:737–739
30. Wang J, Liu ZC, Jiang WY et al (1996) A relationship between susceptibility and grain-size and minerals, and their paleo-environmental implications. Acta Geogr Sin 51:155–163 (in Chinese)
31. JiangYH Yin HF, Wang RH (2004) The theory, method and research progress of environmental magnetism. Acta Geosci Sin 25:357–362 (in Chinese)

32. Tian LL, Deng CL (2001) A brief introduction of rock magnetism. Prog Geophys 16:109–117 (in Chinese)
33. Li JY, Yang JS, Ba DZ et al (2012) Origin of different dunites in the Luobusa ophiolite, Tibet. Acta Petrol Sin 28:1829–1845 (in Chinese)
34. Liang FH, Xu ZQ, Ba DZ et al (2011) Tectonic occurrence and emplacement mechanism of ophiolites from Luobusa-Zedang, Tibet. Acta Petrol Sin 27:3255–3268 (in Chinese)
35. Bai WJ, Zhou MF, Fang QS et al (2000) Diamond and its associated mineral in Luobusa, Tibet. Seismological Press, Beijing (in Chinese)
36. Bai WJ, Fang QS, Zhang ZM et al (1999) The genesis of Luobusa mantle peridotites in the Yarlung Zangbo River ophiolite zone, Tibet. Acta Petrol Miner 18:193–216
37. Bai WJ, Yang JS, Fang QS et al (2001) Study on a storehouse of ultrahigh pressure mantle minerals-podiform chromite deposits. Earth Sci Front 8:111–121 (in Chinese)
38. Zhang HY, Ba DZ, Guo TY et al (1996) Research of Luobusa chromitite deposit in Qusong, Tibet. Tibet Press, Lasa (in Chinese)
39. Wang XB, Bao PS (1987) The genesis of podiform chromite deposits-a case history of the Luobusa chromite deposit, Tibet. Acta Geol Sin 61:166–181 (in Chinese)
40. Wang XB, Zhou X, Hao ZG (2010) Some opinions on further exploration for chromite deposits in the Luobusa area, Tibet, China. Chin Geol Bull 29:105–114 (in Chinese)
41. Zhou MF, Robison PT, Malpas J et al (1996) Podiform chromitites in the Luobusa Ophiolite (Southern Tibet): implications for melt-rock interaction and chromite segregation in the upper mantle. J Petrol 37:3–21
42. Zhou MF, Robinson PT, Malpas J et al (2005) REE and PGE geochemical constraints on the formation of dunites in the Luobusa Ophiolite, Southern Tibet. J Petrol 46:615–639
43. Zhou X, Mo XX, Mahney JJ et al (2001) Sm-Nd dating of gabbro-diabase and Pb, Nd isotopic characteristics of in the Luobusa Ophiolite, Tibet. Chin Sci Bull (Chin Ver) 46:1387–1390 (in Chinese)
44. Li DW (1995) Structural processes of metallogenic evolution of Luobusa chromite deposits. Geosci J Grad Sch CUG 9:450–458 (in Chinese)
45. Ren YF, Chen FY, Yang JS et al (2008) Exsolutions of diopside and magnetite in olivine from mantle dunite, Luobusa Ophiolite, Tibet, China. Acta Geol Sin 82:377–384
46. Yang JS, Dobrzhinetskaya L, Bai WJ et al (2007) Diamond-and coesite-bearing chromitites from the Luobusa ophiolite, Tibet. Geology 35:875–878
47. Liu YX. 3D density and susceptibility rapid inversion based on standard geometric frame. China Patent ZL200810119467.2
48. Yao CL, Zheng YM, Zhang YW (2007) 3-D gravity and magnetic inversion for physical properties using stochastic subspaces. Chin J Geophys 50:1576–1583 (in Chinese)
49. Yao CL, Hao TY, Guan ZN et al (2003) High-speed computation and efficient storage in 3-D gravity and magnetic inversion based on genetic algorithms. Chin J Geophys 46:252–258 (in Chinese)
50. Liu YX, Si HL, Lu YX et al (2009) 3D rapid gravity stripping inversion and its application. In: 71st EAGE conference & exhibition, Amsterdam, The Netherlands, 8–11 June 2009
51. Griffin RH (1995) Geophysical exploration for engineering and environmental investigations. US Army Corps of Engineers
52. Harrison RJ, Dunin-Borkowski RE, Putnis A (2002) Direct imaging of nanoscale magnetic interactions in minerals. Proc Natl Acad Sci USA 99:16556–16561
53. Onyracocne AC (1974) Alteration of chromite from the twin Sisters dunite, Washington. AM Miner 59:608–612
54. Wang XM, Zeng ZG, Ouyang HG et al (2010) Review of progress in serpentinization research of oceanic peridotites. Adv Earth Sci 25:605–616 (in Chinese)
55. Ballhaus C, Berry RF, Green DH (1990) Oxygen fugacity controls in the Earth's upper mantle. Nature 348:437–440
56. Liu CQ, Li HP, Huang ZL et al (2001) A review of studies on oxygen fugacity of the earth mantle. Earth Sci Front 8:73–82 (in Chinese)